IEEESEM

Flood vulnerability assessment of a waste treatment site in Kumasi, Ghana

Frederick Yaw Logah[1]*, Eric Adams[2], Francis Xian Logah[3]

[1]*CSIR Water Research Institute, P. O. Box M.32, Accra, Ghana, [2]Chapman University, Research University in Orange, California – USA, [3]3 Shadowbrook Ln Fredericksburg, VA 22406 - USA

*Correspondence: logahfy@yahoo.com; +233-24-498-8324

ABSTRACT

The study assessed the flood vulnerability of the Asafo Sewerage treatment site within the Kumasi Metropolitan Assembly in Ghana using the HEC-RAS model 1- and 100-year floods. Three distinct scenarios (S1, S2 and S3) relating to the point where the Gee River join the Subin River and another that combined scenario 1 with a built levee (S1+Levee), were tested to ascertain the most effective way of preventing floodwaters from entering the treatment site. The result depicts a direct relationship between flood inundation areas and designed streamflow for the different return periods within the treatment site, with the natural regime already experiencing inundation at least once a year. The observed flood inundation could be due to the low ground elevations and the natural depression created by the diversions of the Gee and Subin Rivers from their natural state within the treatment site. Adopting S2 would increase the extent of inundation from the natural regime by 12.28-19.38% for 1-100-year floods within the treatment site. The results revealed a significant decrease in the 1-year flood extent under S3 (71.58%) and S1+Levee (94.94%), despite a slight rise under S1 (3.24%). The extent of inundations during the 100-year flood was estimated to drop by 38.99%, 40.40%, and 97.01%, S1, S3 and S1+Levee, respectively. The treatment site recorded low flood depths (0.00-0.60 m) and velocities (0.00-1.00 m/s), whilst high flood depths (> 1.0 m) and velocities (> 4.0 m/s) were within the main Subin River channel. It is worth noting that not all the inundated areas within the treatment site are susceptible to high-risk levels, with most of the designated high and very high flood-risk zones located within the main river channels of the Subin and Gee Rivers. The aged, Children, buildings and small vehicles are generally safe within the treatment site due to its low level of susceptibility. Based on the study, S1+Levee is considered the best option to adopt for reducing the amount of flooding within the treatment site, followed by S3 and S1 in that order.

Keywords : Flood vulnerability; Flood extent; High streamflow; Flood risk management; HEC-HMS; HEC-RAS

1 INTRODUCTION

Flooding is a natural phenomenon that constitutes the temporary inundation of territories where people, properties and environmental assets are at risk [1]. Flooding is a major natural disaster that frequently impacts the livelihood and economy worldwide [2], [3], [4]. Flooding is a threat to many parts of the world, with research indicating a rise in the intensity, frequency, and risk of flooding in the coming years with the onset of climate change [5]. Globally, more than 430 catastrophic events were recorded by the Centre for Research on the Epidemiology of Disasters (CRED) in 2021. For the period 2001-2020 (20 years), flooding was the most common natural catastrophe event globally, accounting for over 1.5 billion United States dollars in costs, and it topped all other climate-related disaster events [6], [7], [8].

One of the areas that could pose a high environmental threat if flooded is the waste disposal sites, especially in urban areas where the population is increasing at a higher rate compared to the rate at which flood risk management strategies and infrastructure are being created [8]. As indicated by [9], most waste disposal sites are sited within low-lying areas, flood plains and near coastal areas, which are at risk of being flooded by heavy rain, storm surges and coastal erosion. [10], investigated that about 3,000 landfills in the United Kingdom are located in flood plains and a further 1,264 in low-lying coastal areas [11] stipulated that the exponential increase in the generation and disposal of hazardous waste into landfills may pose dangers to the environment and public health if not properly managed. Siting of hazardous waste facilities is vital in the decision-making process to reduce damage caused by flooding. Sarah in her study [12], proposed a 100-year floodplain as an exclusion zone for the disposal of solid waste.

The poorest and developing countries with low resistance and adaptation capabilities are the most vulnerable to flood. The frequency

Copyright © 2024 IEEE-SEM Publications

of flood occurrences is predicted to increase in Africa due to socioeconomic and climate change issues [13], [14]. Ghana has received lots of international attention through the print and electronic media due to the regular floods that occur every year, usually caused by riverine and flash floods, which affect communities built in the waterways and along the low-lying flat fertile flood plain, which are convenient for farming and other livelihood supports. This information points to the fact that lives are lost and affected, businesses are interrupted, farmlands and critical infrastructures (roads, building footprints, educational and health facilities) are often affected during flooding.

Like many developing countries in sub-Saharan Africa, Ghana faces several challenges regarding the effective way of managing waste produced in its many urban centers because of the country's fast population increase and scarcity of suitable treatment space [15]. Nearly all of Ghana's wastewater treatment plants built in the 1960s and early 1990s, including the one at Kwame Nkrumah University of Science and Technology (KNUST), are broken down as a result of inadequate management [16], [17]. The Asafo wastewater treatment plant, located in Kumasi, the second most populated city in Ghana, is no exception. It was constructed as a pilot project in 1994, broke down in 1997, and was repaired in 2001 [18].

As these facilities break down, untreated sewages from residential areas are released into the surrounding environment. These wastes might affect the yearly reported disease incidence in the city. Studies have indicated that around 55% of the ailments reported in the city of Kumasi are related to water and water-related issues. According to [19], digestive disorders and diarrhoea are among these illnesses.

The Government of Ghana has initiated the construction of new and the rehabilitation of existing wastewater treatment plants in recent years to improve human health and the conditions of the environment. Thus, more households and institutions are expected to benefit from the ongoing expansion and rehabilitation of the Asafo Sewerage Treatment facility within the KMA. Aside from the rehabilitation and construction of the wastewater treatment plants in KMA, flooding within the site can affect human health and pose a danger to environmental health. The Asafo wastewater treatment site is subject to annual flooding, resulting from surface runoffs and bank overflows from the Gee and the Subin Rivers, especially during the wet season. As a result, garbage and eroded materials could be transported to and from the treatment pond. An improper control and management of the treatment site could lead to environmental pollution.

Since 1995, Ghana has seen a rise in the frequency of flooding [20], with global models predicting more land areas to be affected by increased flooding [21]. For early warning, planning and decision-making, a deeper comprehension of the factors contributing to floods is essential. In developing nations like Ghana, rapid and unplanned urbanization, inadequate urban management, inadequate infrastructure, and climate change are some of the causes of floods [6]. Despite the known link of these drivers to flooding, there are inadequate studies that apply hydrology and hydraulic models to assess flood vulnerability and propose measures that could mitigate flood risk at waste disposal sites. In light of the above limitations, this study is being carried out to address some of the measures that can improve human health and environmental conditions through flood mitigation at waste disposal sites using hydrological and hydraulic models. Thus, the objectives of this are to:

i. assess flood vulnerability at the Asafo Wastewater Treatment site that may result from high flood water and
ii. assess flood mitigation scenarios and discuss the best option with low vulnerability and risk within the study site

2 Study Area

The Asafo Sewerage Treatment site, located within the Kumasi Metropolitan Assembly (KMA) in the Ashanti Region of Ghana (Fig. 1), is the chosen area for the study. It lies between latitudes 6°40.002” N to 6°40.010” N and longitudes 1°36.012” W to 1°36.015” W, covering an approximate area of 73,560 m². The treatment site, with an approximate drainage area of 6.08 km², is drained mainly by the Gee and Subin Rivers. The climate in the region is categorized as a wet subequatorial with a bi-modal rainfall pattern, peaking in March-July and September-October. With a total of about 216 raining days in a year, the average annual rainfall amount in Kumasi is about 1244.68 mm, with an average monthly value of 95.74 mm. The mean temperature of the region is approximately 28 °C [22]. Asafo is a residential area within the KMA, covering an approximate area of 2 km² with a resident population of about 20,000 [18, 23]. According to the Minister of Water and Sanitation, the Asafo Sewerage Treatment facility is currently receiving sewerages from 323 households, 13 institutions, and some 14 public latrines within Kumasi [24]. Upon the completion of an ongoing expansion and connecting waste from other facilities, including the Kumasi Central Prisons and the Komfo Anokye Teaching Hospital (KATH), these numbers are expected to double.

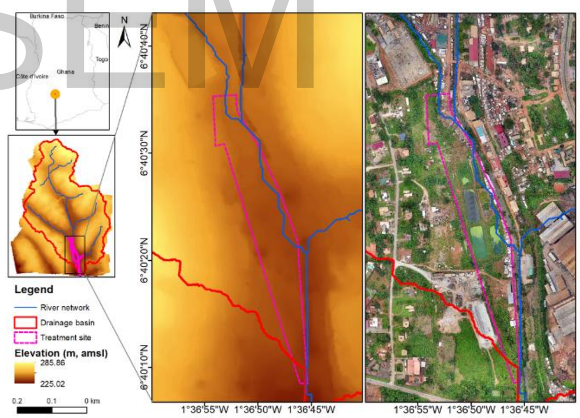

Fig. 1. Study area showing the location of the Asafo treatment site

3 Materials and Methods

3.1 DEM and drainage area

A variety of flood modelling, topographic and natural hazard assessments rely heavily on Digital Elevation Models (DEM) [25], [26]. The resolution of the DEM used for the study is approximately 0.1 x 0.1 m, with elevation values ranging from 225.02-285.86 m above mean sea level (Fig. 2).

3.2 The hydrologic (HEC-HMS) model

Since there were no available gauged streamflow data at or near the study site, a hydrological model was developed for the Pra River Basin at Twifo Praso using the HEC-HMS model. This modelling approach

IEEE-SEM

Copyright © 2024 IEEE-SEM Publications

enabled the consultant to make provisions for extracting streamflow data at the required locations on the Subin River and its tributaries. These values are vital in defining the boundary conditions in the hydraulic model (HEC-RAS). Utilizing the user gauge weighting approach in the HEC-HMS model, the meteorologic model was created using the observed rainfall and streamflow data [27]. The hydrology of the Pra Basin at Twifu Praso was calibrated and validated for the periods 2000–2004 and 2005–2009, respectively, using observed precipitation data for the period 1984–2021. In a later simulation, the model was used to determine stream flows in the river at Subin, Gee, and the tributary close to the treatment site. Fig. 3 shows a schematic illustration of the Pra Basin at Twifu Praso (left) and Subin at the treatment site (right) in the HEC-HMS model. The model's initial parameters were selected using data collected from the literature on the use of HEC-HMS and catchments with similar characteristics [28, 29, 30, 31]. The HEC-HMS model was calibrated and validated at a daily time step using the period and time interval of the observed hydrological data. Three statistical indicators, as summarized in equations 1-3, were used to assess the performance of the HEC-HMS model.

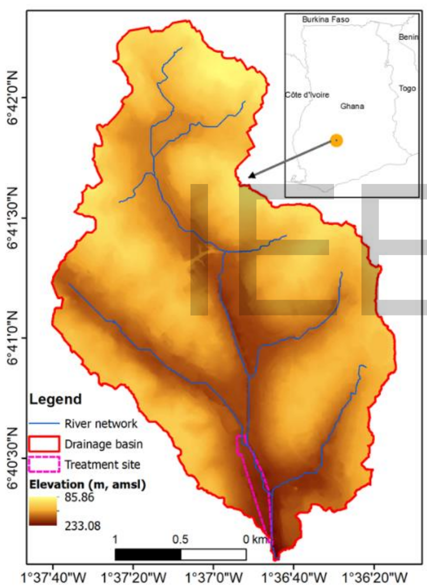

Fig. 2. Drainage of the treatment site

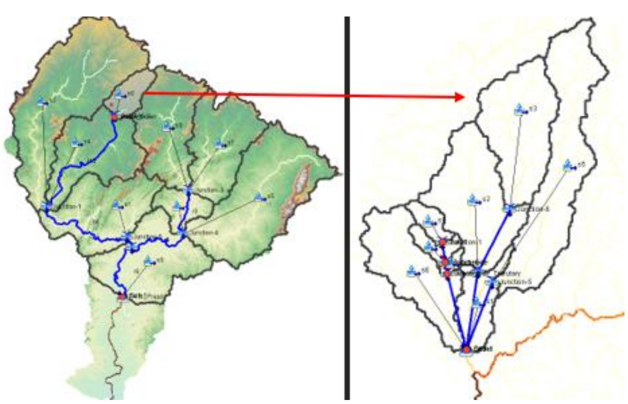

Fig. 3. Schematic representation of the Pra Basin at Twifu Praso (left) and Subin (right)

$$\mathrm{BIAS} = \frac{\sum_{i=1}^{n}(P_i - O_i)}{\sum_{i=1}^{n}(O)} \quad 1$$

$$R = \frac{\sum_{i=1}^{n}(O_i - \bar{O})\sum_{i=1}^{n}(P_i - \bar{P})}{\sqrt{\sum_{i=1}^{n}(O_i - \bar{O})^2 \sum_{i=1}^{n}(P_i - \bar{P})^2}} \quad 2$$

$$\mathrm{NSE} = 1 - \frac{\sum_{i=1}^{n}(P_i - O_i)^2}{\sum_{i=1}^{n}(O_i - \bar{O})^2} \quad 3$$

where R is the Pearson correlation coefficient, NSE is the Nash-Sutcliffe efficiency, $\bar{O}$ and $\bar{P}$ are the means of the observed streamflow (O) and the estimated stream flow (P_i) respectively, and n is the number of compared values.

3.3 Flow duration curve and high flows

The flow duration curve (FDC) was developed for the Subin, Gee and tributary Rivers with daily streamflow data using equation 4 [32], [33]. The section of the FDC which is of most interest to this study is the high streamflow sections of the curve. These were arbitrarily chosen as a part of the curve where flows were exceeded 10 % of the time.

$$P = 100 \times \frac{r}{n+1} \quad 4$$

where P is the percentage of time a given flow is equaled or exceeded, n is the total number of records and r is the rank number for each streamflow with the largest ranked 1 and the smallest n.

3.4 Estimation of return periods for high stream flows

The return period is an important parameter in streamflow research because it describes the likelihood of streamflow events occurring. The extracted high stream flows from the FDC were sorted in descending order of magnitude and assigned rank numbers with the largest ranked 1 and the lowest n. The empirical return period (T_e) for each high streamflow were estimated using equation 5 [32].

$$T_e = \frac{n}{r} \quad 5$$

where r is the rank number for each high streamflow and n is the total duration of the complete streamflow series (in years).

A more simplified extreme value analysis was performed on the extracted high stream flows using the exponential extreme value distribution (EVD). The return periods for the high stream flows were estimated using equation 6 [32]. By rearranging the equation 6 to 7, the designed high stream flow for a specified return period (T-years) was estimated based on linear regressions in the exponential quantile plots.

$$T_c = \frac{n}{t} * \left[1 + \gamma \frac{(x - x_t)}{\beta}\right]^{\frac{1}{\gamma}} \quad 6$$

$$x_T = x_t \frac{\beta}{\gamma}\left[\mathrm{Exp}[\gamma \ln\left(\frac{T_c t}{n}\right)] - 1\right] \quad 7$$

where T_c is the calibrated return period, γ and β are calibrating parameters based on extreme value distribution, t is the number of high streamflows above the threshold value (x_t), n is the total duration of the complete streamflow series (in years) and x_T is the estimated designed high stream flow at T-years.

IEEESEM

Copyright © 2024 IEEE-SEM Publications

3.5 The hydraulic (HEC-RAS) model

Due to its popularity and ease of use across the globe for hydraulic assessment of floods and floodplains [27], [34], [35], the Hydrological Engineering Centre River Analysis System (HEC-RAS) tool was selected for this study. The primary input data of the HEC-RAS model are (i) river geometry, (ii) river floodplain, (iii) the separation between subsequent river cross-sections, (iv) Manning's 'n' value, and (v) boundary conditions. The flood depth, flood velocity, flood extent, and risk level within the treatment site were estimated using the HEC-RAS (version 6.4.1) model. The basic principles in setting up the HEC-RAS model were followed. The normal depth option, which requires so little data was defined for the downstream boundary condition of the river reach with a channel slope of 0.0002 m/m. The unsteady steady state analysis was performed in this study because it corresponds better with evaluating design floods. With the aid of the RAS-MAPPER tool in the HEC-RAS model, the extent of inundation, flood depth, and flood velocity corresponding to 1- and 100-year floods.

3.6 Flood Risk Levels Classification

The frequency, depth, and velocity of floods within a floodplain are all related to the dangers they pose to human life. Therefore, by integrating flood depth and flood velocity, flood risk assessment can be better understood. Flood risk within the study site was assessed at four levels (low, medium, high, and very high) following a modified classification of the Australian Emergency Management Institute (AEMI) guideline 7-3 [36] as outlined in Table 1.

IEEE-SEM

Table 1. Classification and definition of flood risk level (Modified from the AEMI guideline 7-3)

Risk level	Classification values (m^2/s)	Description
Low	≤ 0.30	Generally safe for children, the aged, buildings and small vehicles
Medium	$> 0.30 \leq 0.60$	Unsafe for children and the aged
High	$> 0.60 \leq 1.00$	Unsafe for children, the aged and small vehicles. Can destroy farmland
Very high	> 1.00	Unsafe for vehicles and human. All structures are vulnerable to failure. Farmlands can be destroyed

3.7 Scenarios analyzed

The study tested three scenarios to identify the best option with low-risk flood vulnerability within the treatment site. In the natural regime, the Gee River flows along the boundary and cuts through the middle of the treatment site before joining the Subin River just below the tributary (Fig. 4). As illustrated in Fig. 4, all the scenarios are related to the point where the Gee River joins the Subin River.

Scenario-1 (S1): Changing the direction of the Gee River to join the Subin River from the upper section of the treatment site.

Scenario-2 (S2): Changing the angle at which the Gee River flows into the Subin downstream.

Scenario-3 (S3): Combining scenario-1 and the natural regime such that 50% of the flow in the Gee River joins the Subin River upstream of the treatment site and the remaining 50% flow through the natural regime

In each case, an approximate excavated depth of 1.25 m was considered from the point of diversion of the Gee River to the Subin River

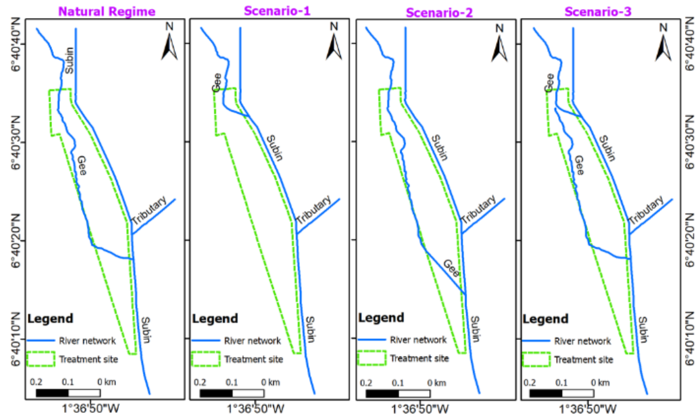

Fig. 4. Natural River network and scenarios considered in the study

3.8 Special case scenario

A hypothetical situation in which a levee is built to prevent high floodwaters from entering the treatment site was modelled and simulated with the HEC-RAS model. Depending on where the Gee River joins the Subin River, S1 was considered the appropriate option to adopt with the built levee (S1+levee). As illustrated in Fig. 5, the levee was modelled along the boundary of the treatment site to keep high floodwaters from the Gee and Subin Rivers from entering the treatment site. The height or elevation of the levee along the treatment site was estimated to be about 0.2 m more than the water surface elevation data gathered in the study. The impacts of floods caused by the constructed levee within the treatment site and the nearby environs were assessed.

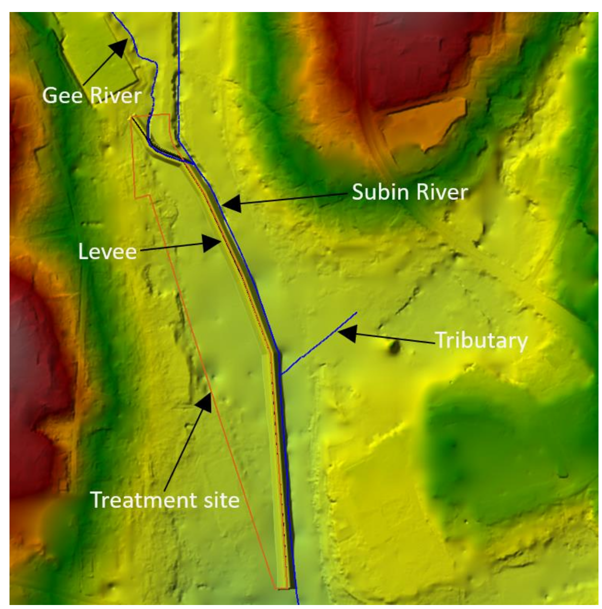

Fig. 5. A representation of the scenario 1 with the built levee along the boundary of the treatment site

Copyright © 2024 IEEE-SEM Publications

4.0 Results and Discussions

4.1 Digital elevation model and drainage

The total drainage area contributing to the Subin River at the treatment site is approximately 6.08 km². Fig. 6 compares the river network generated from the DEM and the existing networks of the Gee and Subin Rivers at the treatment site. It can be observed from Fig. 6 that there is a mismatch between the two river networks at the treatment. From the existing condition on the ground, the Subin River does not flow through the treatment site, whereas the Gee River flows along the bank of the treatment site before joining the Subin River. The DEM-generated river network indicates that the Gee River joins the Subin River within the upper section of the treatment site, which then flows within the treatment site near the boundary before exiting just around the middle of the treatment site. The mismatch between the river networks could be because both the channels of the Gee and the Subin Rivers were recreated and diverted in the past from their natural (generated river network) to the current path at the site.

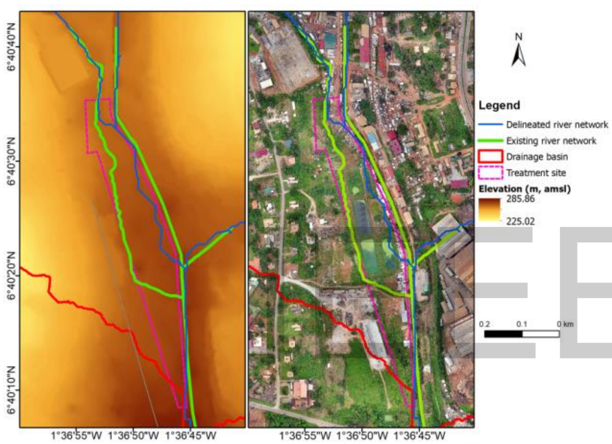

Fig. 6. Comparison between generated and exiting river network at the study site

4.2 HEC-HMS model calibration and validation

The performance of the HEC-HMS model in simulating daily streamflow at Twifo Praso is graphically illustrated in Fig. 7 under calibration and validation periods. The simulated streamflow values (0.03-920.00 m³/s) were well within the range of the observed streamflow (0.30-1,040.10 m³/s), with the results showing a satisfactory fit between simulated and observed stream flows, resulting in a good NSE (0.50-0.66), high coefficient of correlation ($R \geq 0.78$) and a satisfactory model bias ($\leq$ -0.13) values during the simulation period. The model successfully captured the peak flows, which are essential for flood analysis, over the simulation period. The performance of the HEC-HMS model could be considered satisfactory in simulating streamflow in the Pra Basin.

The daily streamflow values extracted from the model at the required locations on the Subin River and its tributaries are presented in Fig. 8 for the period 1984-2021, with values ranging from 0.10-10.18 m³/s, 0.00-2.21 m³/s, and 0.00-0.50 m³/s in the Subin, Gee, and tributary Rivers, respectively. The mean stream flow values from these rivers are approximately 0.25 m³/s, 0.05 m³/s, and 0.02 m³/s, respectively.

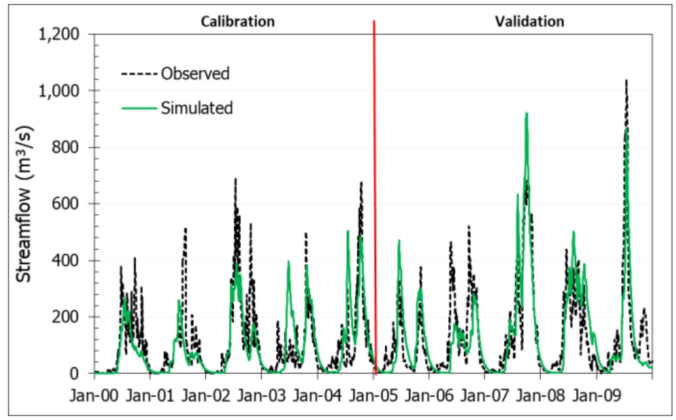

Fig. 7. Simulated daily streamflow at Twifo Praso in the Pra River Basin in Ghana.

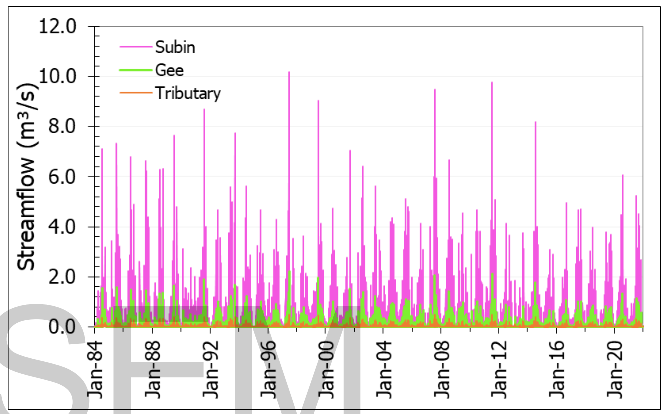

Fig. 8. Daily streamflow in the Subin River and its tributaries for the period 1984-2021

4.3 Designed flows for different return periods

Fig. 9 illustrates the flow duration curve developed for the Subin, Gee and the Tributary Rivers in the study area with the threshold values above which these flows are considered high flows are estimated at 10% probability of exceedance to be approximately 0.66 m³/s, 0.14 m³/s and 0.04 m³/s, respectively.

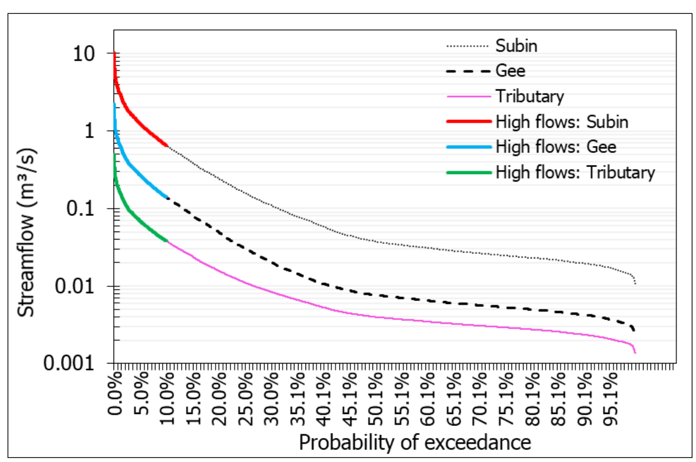

Fig. 9. Flow Duration curves developed for the Subin River and its tributaries

IEESEM

Copyright © 2024 IEEE-SEM Publications

Fig. 10 illustrates the recurrent intervals of high streamflow at Subin, Gee, and the tributary Rivers, with the estimated results indicating that high stream flow values of 4.73 m^3/s & 10.82 m^3/s, 1.03 m^3/s & 2.5 m^3/s, and 0.25 m^3/s & 0.56 m^3/s are expected to occur at least once every 1- & 100-year, respectively.

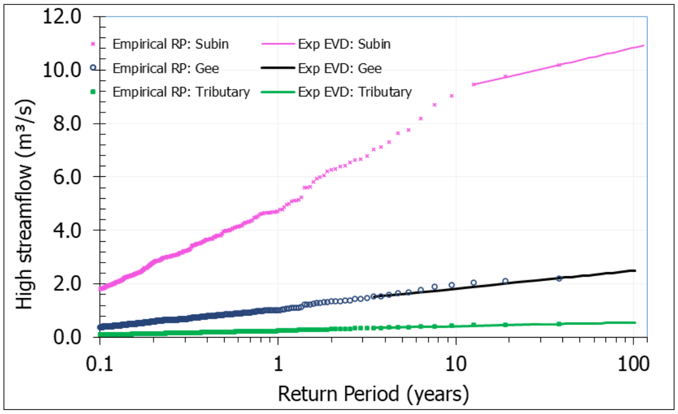

Fig. 10. Return period of stream flows developed for the Subin River and its tributaries

4.4 Extent of inundation

Figs. 11 and 12 compares the extent of inundation between the natural regime, scenario-1 (S1), scenario-2 (S2) and scenario-3 (S3) using an average excavated depth of 1.25 m from the point of diversion to the point where the Gee River joins the Subin River for 1- and 100-year floods, respectively. Fig. 13 on the other hand compares the flood extents between the natural regime and the one with the combined scenario-1 and the built levee (S1+Levee). The result depicts a direct relationship between inundated areas and designed streamflow for the different return periods (Table 2).

The natural regime already experiences inundation with the 1- and 100-year floods covering about 28.25% (20,778.06 m²) and 52.36% (38,518.70 m²) of the treatment site, respectively; indicating that the 100-year flood in the natural regime will inundate about 46.06% more area than the 1-year flood within the treatment site. The observed inundation could be due to the low ground elevations within the treatment site and the natural depression created by the diversions of the Gee and Subin Rivers from their natural state.

In all the scenarios, the extent of inundation was estimated to increase from the natural regime by 19.38% and 12.28% under S2 for the 1- and 100-year floods, respectively. Though, there is a marginal increase under S1 (3.24%), the results on the other hand showed an immense reduction in the 1-year flood extent under the scenario-3 (71.58%) and the S1+Levee (97.01%). For the 100-year flood, the extent of inundation was estimated to decrease under S1, S3 and S1+Levee by 38.99%, 40.40% and 94.94%, respectively. These results suggest that portions of the treatment site would still flood during heavy flows even after the construction of the levee. These 1-100-year flood covering about 2.99-5.06% of the treatment site, were observed to be occurring at the (i) top upper right portion of the treatment site, which is not protected by the levee to allow the Gee River to flow freely into the Subin River and (ii) lower end of the treatment site which is inundated due to backwater effect. Even though the overall extent of inundation has improved within the treatment site under S1+levee, it has resulted in an increased inundation extending away from the left bank of the Subin River (Fig. 13). The extended inundated area extending from the built levee is estimated to cover an extra area of $5.53 \times 10^{-3} - 11.88 \times 10^{-3}\ km^2$ approximately.

IEEE SEM

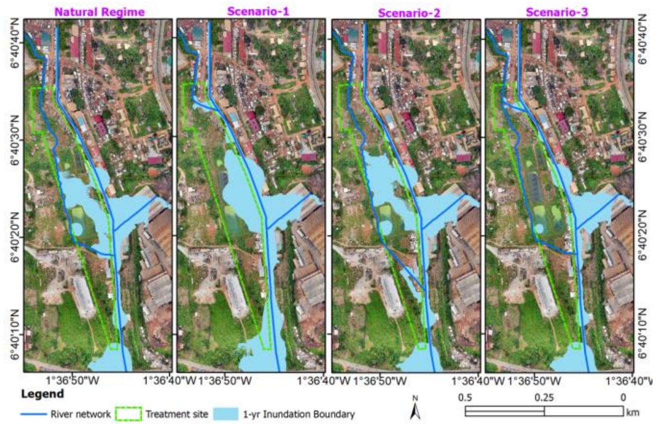

Fig. 11. Inundation boundaries for 1-year floods

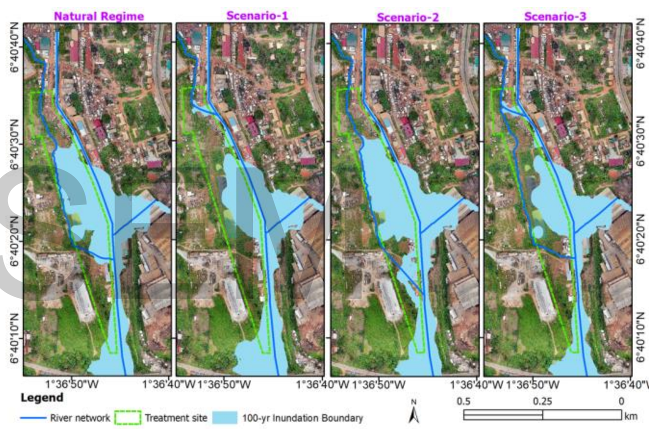

Fig. 12. Inundation boundaries for 100-year floods

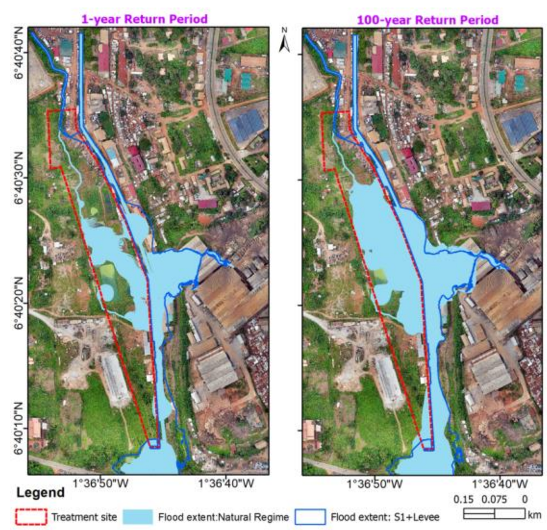

Fig. 13. Comparison of 1- (left) and 100-year (right) flood extents between the natural regime and S1+Levee

Copyright © 2024 IEEE-SEM Publications

Table 2. Inundated areas and percentage change under S1, S2, S3 and S1+Levee within the treatment site

Return period (years)	Extent of inundation (m^2)	Change in inundation extent (%)			
		S1	S2	S3	S1+Levee
1	20,778.06	3.24	19.38	-71.58	-97.01
100	38,518.70	-38.99	12.28	-40.40	-94.94

4.5 Elevation, length and slope of levee

Fig. 14 (up) compares the elevations on the ground (236.6-245.9 m, asl) and levee (239.0-244.9 m, asl), while Fig. 14 (down) shows the height of the levee above the ground level, along the boundary of the treatment site. The total length of the levee is approximately 956.0 m, with an approximate slope of 0.0003 m/m. Depending on the elevations along the boundary of the treatment site, the height of the levee above the ground ranges from 0.0-3.2 m with a mean value of 1.5 m.

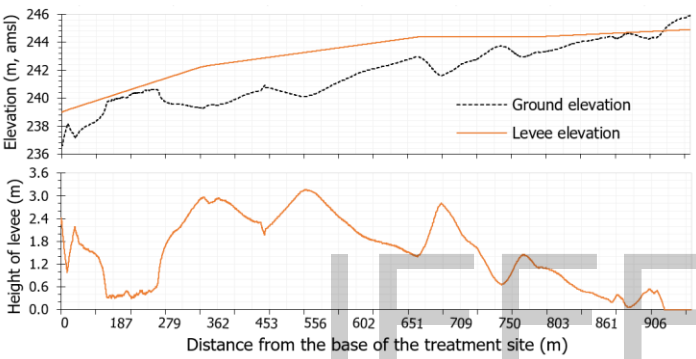

Fig. 14. Elevation of the ground and height of the levee along the boundary of the treatment site

4.6 Inundation depth, velocity and WSE

Figs. 15-17 illustrate the variations in flood depths, flood velocities, and water surface elevations (WSE), respectively for 1- and 100-year floods. The simulated flood depths range from 0.00-4.09 m and 0.00-4.32 m for 1- and 100-year floods, respectively (Fig. 15) while the distribution of flood velocities ranged from 0.00 m/s to more than 4.00 m/s, respectively (Fig. 16). The vast majority of the flood depths and velocities within the treatment site are minimal, with values ranging from 0.00-0.60 m and 0.00-1.00 m/s, respectively. The deepest flood depths (> 1.0 m) and high flood velocities (> 4.0 m/s) were observed to be within the main Subin River channel. The WSE values were simulated to range from 235.00-244.10 m and 235.30-244.50 m for the 1- and 100-year floods, respectively (Fig. 17).

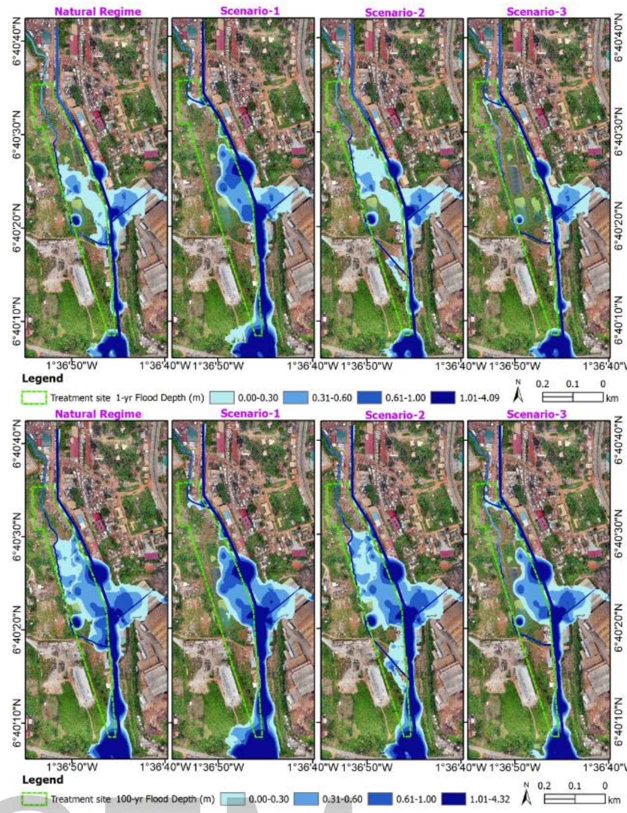

Fig. 15. Depths for 1- (up) and 100-year (down) floods

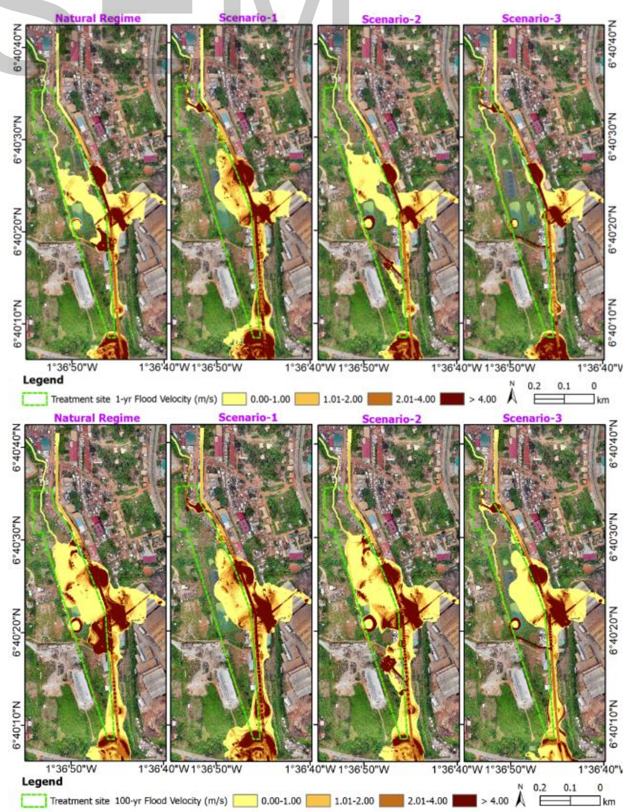

Fig. 16. Velocities for 1- (up) and 100-year (down) floods

IEEE-SEM

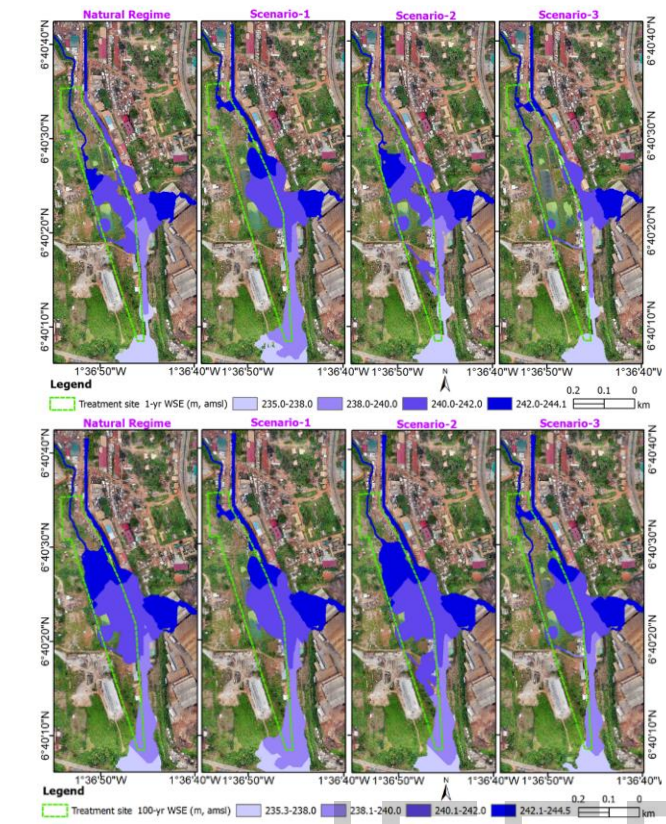

Fig. 17. WSE for 1- (up) and 100-year (down) floods

4.7 Vulnerability to flood

Fig. 18 shows the flood risk maps generated for the study site for 1- and 100-year floods. It is important to note that not all the inundated areas within the treatment site are susceptible to high-risk levels resulting from the 1-100-year floods. Most of the areas designated as high and very high-risk flood risk levels are located within the main river channels of the Subin and Gee Rivers. Thus, the level of vulnerability within the treatment site falls within the low-risk flood zone with values ranging between 0.00-0.30 m²/s, which is generally safe for children, the elderly, buildings and small vehicles.

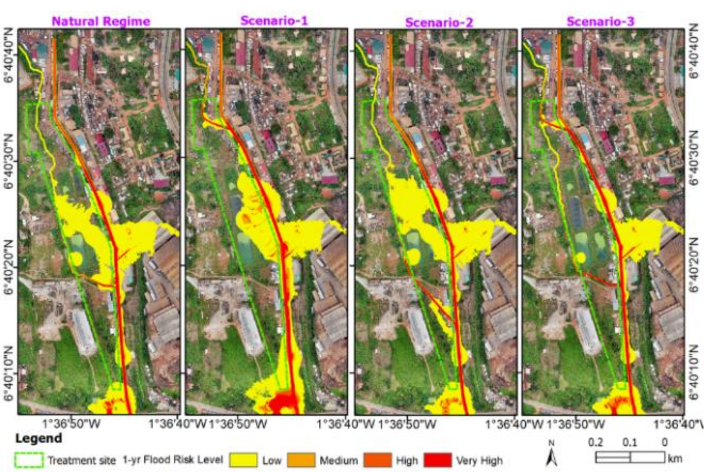

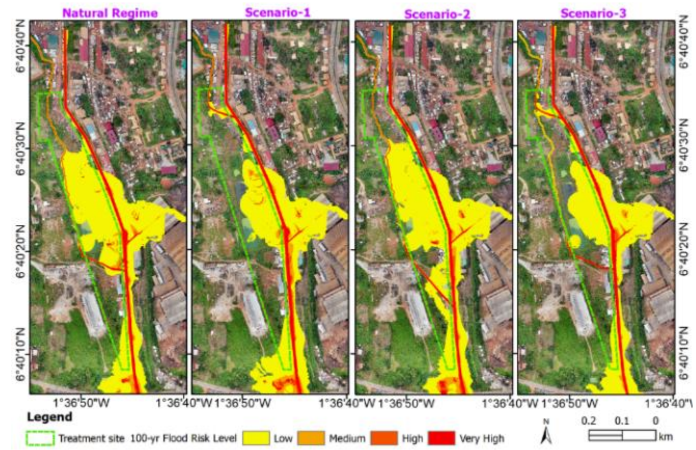

Fig. 18. Flood Risk levels for 1- (up) and 100-year (down) floods

4.8 WSE, depth, velocity and flood risk level emanating from the built levee

In the special case scenario, Fig. 19 illustrate the estimated SWE, flood depth, flood velocities and flood risk level within the treatment site which were simulated with a levee built along the boundary of the treatment site under scenario-1 (S1+levee) for 1- (up) and 100-year (down) floods. The simulated water surface elevation corresponding to 1-00-year floods was estimated to range from 235.5-244.3 m. The simulated flood depth and flood velocity under S1+Levee range from 0.00-5.14 m and 0.00 - > 4.00 m/s, respectively. The deepest flood depths (≥ 1.0 m) and high flood velocities (> 4.0 m/s) are within the main Subin River channel. Since the treatment site is saved from flood water, almost all flood risk levels (low-very high flood risk level) are located within the main Subin River channel and along the built levee along the treatment site. Thus, there is no level of vulnerability within the treatment site due to the built levee. From the analysis, S1+Levee is considered the best option to adopt concerning the reduction in the extent of flood inundation within the treatment site, followed by S3 and S1 in that order.

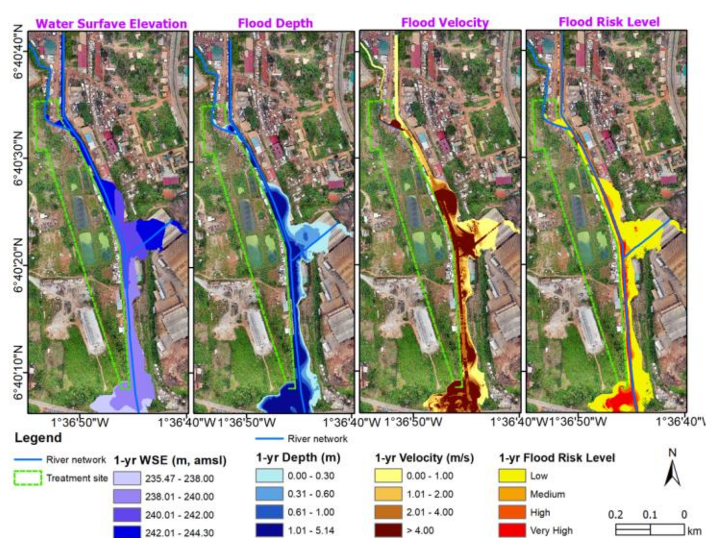

IEEE-SEM

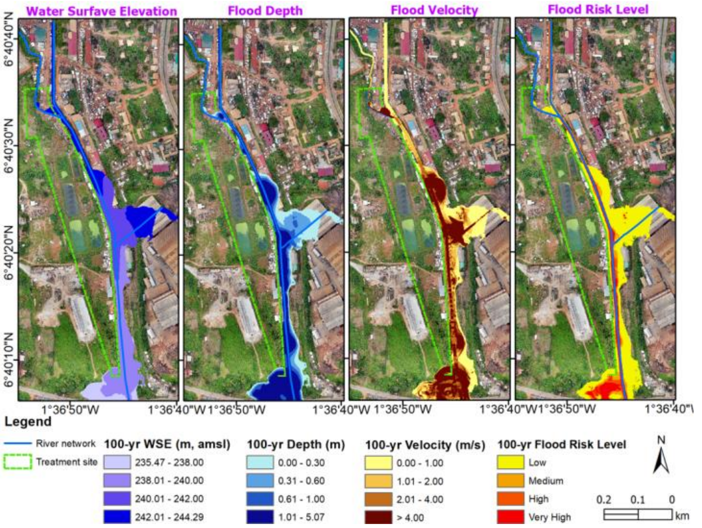

Fig. 19. Comparison of 1- (up) and 100-year (down) WSE, flood depths, flood velocities and flood risk levels under S1+Levee

5 Conclusions and Recommendations

With designed stream flows of 1- and 100-year return periods, the HEC-RAS model was used to evaluate the vulnerability of the Asafo Sewerage treatment facility located in Ghana's second most populous region. To determine the most efficient method of keeping floodwaters from entering the treatment site, three (3) distinct scenarios (S1, S2, and S3) related to the point of confluence between the Gee and Subin Rivers and another, which merged scenario 1 with a built levee (S1+Levee), were investigated.

Based on the low ground elevations and the natural depression formed by the Gee and Subin Rivers' diversion from their natural state within the treatment site, the results show that flood inundation happens at least once a year. The results revealed a significant decrease in the 1-year flood extent under S3 (71.58%) and S1+Levee (94.94%), despite a slight rise under S1 (3.24%). Under S1, S3, and S1+Levee, the extent of flood inundation within the treatment site is predicted to decrease by 38.99%, 40.40%, and 97.01%, respectively, during the 100-year flood.

It is worth noting that not all the inundated areas within the treatment site are susceptible to high-risk flood levels, with most of the designated high and very high flood-risk zones located within the main channels of the Subin and Gee Rivers. Thus, the level of vulnerability within the treatment site is low, which is generally safe for children, elderly, buildings and small vehicles. According to the analysis, S1+Levee is considered the best option to adopt concerning reduction in the extent of flood inundation within the treatment site, followed by S3 and S1 in that order.

References

[1] S. Asumadu-Sarkodie, A. Owusu Phebe, and C. Jayaweera Herath M P, "Flood risk management in Ghana: A case study in Accra," Adv. Appl. Sci. Res., vol. 6, no. 4, pp. 196–201, 2015, [Online]. Available: www.pelagiaresearchlibrary.com

[2] O. Rosane, "Flooding 101: Everything you need to know." Accessed: Jan. 12, 2023. [Online]. Available: https://www.ecowatch.com/flooding-facts-ecowatch.html

[3] A. Asante-Annor, E. Ansah, and K. Acherefi, "Preliminary Flood Vulnerability and Risk Mapping of Koforidua and its Environs using Integrated Multi-Parametric AHP and GIS," pp. 91–102, 2020.

[4] Y. O. Ouma and R. Tateishi, "Urban flood vulnerability and risk mapping using integrated multi-parametric AHP and GIS: Methodological overview and case study assessment," Water (Switzerland), vol. 6, no. 6, pp. 1515–1545, 2014, doi: 10.3390/w6061515.

[5] S. N. Jonkman and R. J. Dawson, "Issues and challenges in flood risk management-Editorial for the special issue on flood risk management," Water (Switzerland), vol. 4, no. 4, pp. 785–792, 2012, doi: 10.3390/w4040785.

[6] A. J. Echendu, "Flooding and Waste Disposal Practices of Urban Residents in Nigeria," GeoHazards, vol. 4, no. 4, pp. 350–366, 2023, doi: 10.3390/geohazards4040020.

[7] O. Rosane, "2023's costliest weather disasters reveal 'double ineequality' of climate crisis." Accessed: Jan. 12, 2023. [Online]. Available: https://www.commondreams.org/news/2023-costliest-weather-disasters

[8] O. A. Mokuolu, A. K. Odunaike, J. O. Iji, and A. S. Aremu, "Assessing the Effects of Solid Wastes on Urban Flooding: A case study of Isale Koko," LAUTECH J. Civ. Environ. Stud., vol. 9, no. 1, pp. 22–30, 2022, doi: 10.36108/laujoces/2202.90.0130.

[9] E. Wille, "Flooding risks at old landfill sites: Linear economy meets climate change," Proc. 4th Int. Symp. Enhanc. landfill Min., pp. 361–365, 2018, [Online]. Available: https://www.nweurope.eu/media/3964/elfm-iv-rawfill-1.pdf%0Ahttps://www.semanticscholar.org/paper/FLOODING-RISKS-AT-OLD-LANDFILL-SITES%3A-LINEAR-MEETS-Wille/5f2c2ef8552d3ef64c64789ddf71995fde09c4d3

[10] K. Vasarhelyi, "The hidden damage of landfills," Environental Center, Division of sttudent affairs. Accessed: Jan. 05, 2023. [Online]. Available: https://www.colorado.edu/ecenter/2021/04/15/hidden-damage-landfills

[11] G. Ozbay, M. Jones, M. Gadde, S. Isah, and T. Attarwala, "Design and Operation of Effective Landfills with Minimal Effects on the Environment and Human Health," J. Environ. Public Health, pp. 1–13, 2021, doi: https://doi.org/10.1155/2021/6921607.

[12] M. Sara, "Site assessment and remediation handbook," Lewis Publication, 2003.

[13] A. J. Echendu, "Women, Development, and Flooding Disaster Research in Nigeria: A Scoping Review," Environ. Earth Sci. Res. J., vol. 8, no. 4, pp. 147–152, 2021, doi: 10.18280/eesrj.080401.

[14] E. Merz, B.; Blöschl, G.; Vorogushyn, S.; Dottori, Francesco; Aerts, Jeroen C.J.H; Bates, Paul; Bertola, Miriam; Kemter, Matthias; Kreibich, Heidi; Lall, Upmanu; Macdonald, "Causes, impacts and patterns of disasterous river floods," Nat Rev Earth Env., vol. 2, pp. 592–609, 2021, doi: https://doi.org/10.1038/s43017-021-00195-3.

[15] M. L. Graham, J.; Polizzotto, "Pit laterines and their impacts on groundwater quality: a systematic review," Environ. Health Perspect., vol. 121, pp. 521–530, 2013.

[16] E. Monney, I.R.; Boakye, R.; Buamah, R.; Anyemedu, F.O.K.; Odai, S.N.; Awuah, "Urbanisation and polution of surface water

resources in the two largest cities in Ghana.," Int. J. Environ. Monit. Anal, vol. 1, pp. 279–287, 2013.
[17] L. Y. Salifu, "Sewerage maintenance management in Ghana.," in Water and Sanitation for all-partnerships and innovations, Durban, South africa: Preceedings of the 23rd WEDC conference, 1997, pp. 84–87.
[18] H. Awuah, Esi; Amankwaah-Kuffour, Richard; Fosu Gyasi, Samuel; J. Lubberding, "Characterisation and Management of Domestic WW in two Suburbs of Ghana," Res. J. Environ. Sci., vol. 8, no. 6, pp. 318–330, 2014, doi: 10.3923/rjes.2014.318.330.
[19] E. Owusu-Sekyere, E. Harris, and E. Bonyah, "Forecasting and Planning for Solid Waste Generation in the Kumasi Metropolitan Area of Ghana: An ARIMA Time Series Approach," Int. J. Sci., vol. 2, no. 04, pp. 69–83, 2013, [Online]. Available: https://www.ijsciences.com/pub/article/179%0Ahttps://doi.org/%0Ahttps://www.ijsciences.com/pub/pdf/V2-201304-17.pdf
[20] S. O. Ansah et al., "Meteorological Analysis of Floods in Ghana," Adv. Meteorol., vol. 2020, 2020, doi: 10.1155/2020/4230627.
[21] IPCC, "10 big findings from the 2023 IPCC report on climate change," Washinton DC, Mar. 2023. [Online]. Available: https://www.wri.org/insights/2023-ipcc-ar6-synthesis-report-climate-change-findings
[22] W. and Climate, "The global historical weather and climate weather," Kumasi, Ghana, 2024. [Online]. Available: https://weatherandclimate.com/ghana/ashanti/kumasi
[23] T. Ghanaian, "Asafo sewerage system to be expanded to cover 500 households, 29 institutions," Accra, Ghana, p. 1, Jun. 27, 2023. [Online]. Available: https://www.ghanaiantimes.com.gh/asafo-sewage-system-to-be-expanded-to-cover-500-households-29-institutions/#:~:text=The Asafo sewage system is, making up about 20%2C000 people.
[24] GNA, "Asafo sewerage treatment facility expansion to serve more people," Ghana News Agency, Accra, Ghana, p. 1, Jan. 20, 2023. [Online]. Available: https://gna.org.gh/2023/06/asafo-sewage-treatment-facility-expansion-to-serve-more-people/
[25] U. Khalil, N. M. Khan, and Habib-ur-Rehman, "Floodplain mapping for Indus River: Chashma -Taunsa Reach," Pakistan J. Eng. Appl. Sci., vol. 20, pp. 30–48, 2017.
[26] M. S. Khattak, F. Anwar, T. U. Saeed, M. Sharif, K. Sheraz, and A. Ahmed, "Floodplain Mapping Using HEC-RAS and ArcGIS: A Case Study of Kabul River," Arab. J. Sci. Eng., vol. 41, no. 4, pp. 1375–1390, 2016, doi: 10.1007/s13369-015-1915-3.
[27] USACE, "Hydrologic Modeling System HEC-HMS, User's Manual.," Hydrol. Eng. Cent., vol., no. Version 4.3, p. 640, 2018, [Online]. Available: https://www.hec.usace.army.mil/software/hec-hms/documentation/HEC-HMS_Users_Manual_4.3.pdf
[28] F. Y. Logah, E. Obuobie, K. A. Adjei, C. Gyamfi, and S. N. Odai, "Capability of satellite rainfall products in simulating streamflows in the Black Volta Basin," Sustain. Water Resour. Manag., vol. 9, no. 3, 2023, doi: 10.1007/s40899-023-00871-w.
[29] W. Agyekum, A. A. Duah, C. Okra, and E. Manu, Groundwater recharge studies and trends in the Lower Volta River Basin, Ghana., In. Dams, development and downstream communities: Implications for re-optimising the operations of the Akosombo and Kpong dams in Ghana., 2017.
[30] O. F. Mensah, C. Alo, and S. M. Yidana, "Evaluation of groundwater recharge estimates in a partially metamorphosed sedimentary basin in a tropical environment: Application of natural tracers," Sci. World J., vol. 2014, 2014, doi: 10.1155/2014/419508.
[31] V. Thiemig, R. Rojas, M. Zambrano-Bigiarini, and A. De Roo, "Hydrological evaluation of satellite-based rainfall estimates over the Volta and Baro-Akobo Basin," J. Hydrol., vol. 499, pp. 324–338, 2013, doi: https://doi.org/10.1016/j.jhydrol.2013.07.012.
[32] P. Willems, "Statistic for Water Engineering, Lecture note. Katholieke Universiteit Leuven (KULeuven), Leuven, Belgium.," Katholieke Universiteit Leuven (KULeuven), Leuven, Belgium., 2007.
[33] V. Smakhtin, "Low Flow Hydrology: A review," J. Hydrol., vol. 240, no. 3–4, pp. 147–186, 2001, doi: 10.1016/S0022-1694(00)00340-1.
[34] S. Ogras and F. Onen, "Flood Analysis with HEC-RAS: A Case Study of Tigris River," Adv. Civ. Eng., vol. 2020, 2020, doi: 10.1155/2020/6131982.
[35] H. S. Mashriqui, J. S. Halgren, and S. M. Reed, "1D river hydraulic model for operational flood forecasting in the tidal Potomac: evaluation for freshwater, tidal, and wind-driven events," J. Hydraul. Eng., vol. 140, no. 5, p. 04014005, 2014, doi: 10.1061/(ASCE)HY.1943-7900.0000862.
[36] Australian Emergency Management Institute [AEMI], "Technical flood risk management guideline: Flood hazard," Aust. Inst. Disaster Resil. CC BY-NC, p. 34 pages, 2014.

IEEE-SEM

Copyright © 2024 IEEE-SEM Publications